

Theory of Network Catalyzer Dynamics for the Thermodynamic Properties of Two-dimensional Quantum Lattice Models

Shi-Ju Ran, Bin Xi, Tao Liu and Gang Su*

*Theoretical Condensed Matter Physics and Computational Materials Physics Laboratory,
School of Physics, University of Chinese Academy of Sciences, P. O. Box 4588, Beijing 100049, China*

We develop a nonlinear dynamic theory based on the tensor network state representation that is termed as network catalyzer dynamics (NCD) to explore the thermodynamic properties of two-dimensional quantum lattice models. An imaginary-time-sweep algorithm for implementation of the NCD method is proposed for practical numerical simulations. The results obtained by the NCD are disclosed nicely in agreement with the quantum Monte Carlo calculations. The quasi-entanglement entropy S , Lyapunov exponent I^{ly} and loop character I^{loop} are introduced within the dynamic scheme, which are found to display the “nonlocality” near the critical point, and can be good characters to detect the thermodynamic phase transitions.

PACS numbers: 75.10.Jm, 75.40.Mg, 05.30.-d, 02.70.-c

The two-dimensional (2D) strongly correlated quantum models have triggered broad interest in last decades as they always exhibit intriguing and exotic properties such as fractional quantum Hall effect [1] and quantum spin liquid state [2], etc. Accompanied with the boom of quantum information science, new theories [3, 4] enable us to describe the critical phenomena beyond the traditional paradigm of Landau-Ginzburg and renormalization group and access the information of phase transitions by studying the properties of quantum states without acquiring knowledge of order parameters or universality class. Owing to the complexity of many-body interactions, reliable and controllable analytical methods for these systems are still sparse, and numerical means thus play essential roles. Among others, the quantum Monte Carlo (QMC), density matrix renormalization group (DMRG) [5] as well as its variants [6, 7], tensor network state (TNS) based algorithms [8–11, 15], and so on, have achieved great success [12, 13]. However, QMC is not applicable to the frustrated spin systems and Hubbard model away from the half-filling because of the “negative sign” problem, and DMRG is remarkably accurate and efficient in one dimension but has great costs for 2D systems of large size. Therefore, to develop new theories and efficient algorithms for correlated quantum lattice systems is highly encouraged.

In this Letter, we develop a nonlinear dynamic theory with the TNS representation of the density operator, termed as the network catalyzer dynamics (NCD), for exploring the thermodynamic properties of the infinite 2D quantum spin lattice models. The partition function as well as the averages of observable operators can be expressed in a simple form with the cell tensor and the corresponding catalyzers that can be obtained through a dynamic way. Within the framework of the NCD, the quasi-entanglement entropy S defined by the transfer matrix of the partition function, Lyapunov exponent I^{ly} that quantifies the convergent properties and loop character I^{loop} for the loop dependence are introduced to describe the properties of the TNS. An imaginary-time-sweep algorithm that is free from the negative sign problem for implementation of the NCD method is proposed. The results calculated by the NCD for the spin-1/2 Heisenberg antiferromagnet (HAF) on

honeycomb lattice are nicely compared with the QMC simulations, showing the efficiency and accuracy of such a method. The quantities S , I^{ly} and I^{loop} are revealed to be able to detect possible thermodynamic phase transitions of the system, which are all characterized by sharp peaks at critical points, as manifested by the spin-1/2 anisotropic honeycomb HAF model as an example.

Tensor network state representation for the density operator.— Suppose that the Hamiltonian can be written as $\hat{H} = \sum_{\langle ij \rangle} \hat{H}^{ij}$, where \hat{H}^{ij} is the local Hamiltonian of two connected spins at i th and j th lattice sites. Without losing generality, we take the infinite honeycomb lattice as the prototype here. Let us begin with introducing the local evolution operator $\hat{U}^{ij} = e^{-\tau \hat{H}^{ij}} = \sum_{p_i p_j p'_i p'_j} U_{p_i p_j p'_i p'_j} |p_i p_j\rangle \langle p'_i p'_j|$, where τ is the infinitesimal imaginary time slice, $|p_i\rangle$ is the local basis of the i th spin and p_i is called the physical bond. By using the Trotter-Suzuki decomposition [14], we can write the density operator at inverse temperature β as $\hat{\rho}(\beta) = [\prod_{\langle ij \rangle} \hat{U}^{ij}]^K$ with $\beta = K\tau$. Define the evolution tensors \mathbf{G}^L and \mathbf{G}^R as $G_{p_i p'_i, g}^L = U_{p_i p'_i, g}^L \sqrt{\lambda_g}$ and $G_{p_j p'_j, g}^R = U_{p_j p'_j, g}^R \sqrt{\lambda_g}$, where $U_{p_i p'_i, g}^L$ ($U_{p_j p'_j, g}^R$) contains the left (right) singular vectors and λ_g contains the singular values of the matrix $U_{(p_i p'_i)(p_j p'_j)}$. We call g the geometrical bond. Then the partition function is represented as the contraction of a closed tensor network (TN), which is a three-dimensional brick-wall structure formed by \mathbf{U}^L 's and \mathbf{U}^R 's. Obviously, it is impossible to complete such a contraction exactly. One way to do this is first to construct the tensor product density operator (TPDO) [15] at inverse temperature τ as $\rho(\tau) = gTr(\prod_{i=odd} \mathbf{A}^i \prod_{j=even} \mathbf{B}^j)$ with $A_{p_i p'_i, g_a g_b g_c}^i = \sum_{p''_i p'''_i} G_{p_i p''_i, g_a}^L G_{p''_i p'_i, g_b}^L G_{p'_i p'''_i, g_c}^L$, $B_{p_j p'_j, g_a g_b g_c}^j = \sum_{p''_j p'''_j} G_{p_j p''_j, g_a}^R G_{p''_j p'_j, g_b}^R G_{p'_j p'''_j, g_c}^R$, and then to evolve the TPDO as $\tilde{A}_{p_i p'_i, g_a g_b g_c}^i = \sum_{p'_i} A_{p_i p'_i, g_a g_b g_c}^i G_{p'_i p'_i, g'_a}^L$ with the composite index $\tilde{g}_a = (g_a, g'_a)$ while keeping its form unchanged (the contractions of \mathbf{B}^j and \mathbf{G}^R are similar). The gTr means summing over all shared geometrical bonds. During the evolution, the geometrical bonds will be enlarged exponentially with the contractions, and proper approximations are needed to bound their dimensions.

Network catalyzer dynamics.— Denote β as the inverse temperature of the present TPDO $\hat{\rho}(\beta)$, and $(\beta + \beta')$ is the targeted inverse temperature. The partition function may be rewritten as $Z(\beta + \beta') = \text{Tr}[\hat{\rho}(\beta)\hat{\rho}(\beta')]$. Suppose that we also have the TPDO representation of $\hat{\rho}(\beta')$ that is comprised of $\tilde{\mathbf{A}}$'s and $\tilde{\mathbf{B}}$'s. Consequently,

$$Z(\beta + \beta') = p\text{Tr}[g\text{Tr}(\prod_{i=\text{odd}} \mathbf{A}^i \prod_{j=\text{even}} \mathbf{B}^j)g\text{Tr}(\prod_{\tilde{i}=\text{odd}} \tilde{\mathbf{A}}^{\tilde{i}} \prod_{\tilde{j}=\text{even}} \tilde{\mathbf{B}}^{\tilde{j}})] \prod_k (\delta^k, \tilde{\delta}^k) \quad (1)$$

where $p\text{Tr}$ stands for summing over all shared physical bonds, δ^k and $\tilde{\delta}^k$ are the Dirichlet matrices with elements $\delta_{p'_k p_k}$ and $\tilde{\delta}_{\tilde{p}'_k \tilde{p}_k}$, respectively.

Now we define the catalyzable closed TN of the partition function with the following two restrictions: (a) The TN is formed only by one inequivalent tensor that is called the cell tensor and denoted as \mathbf{T}^{cell} . The cell tensor may be chosen as a small cluster that consists of several properly selected original tensors. Straightforwardly, a new larger cell tensor can be constructed by a cluster of cell tensors. We denote $\mathbf{T}^{\text{cell}(1)}$ as the smallest cell tensor and $\mathbf{T}^{\text{cell}(\gamma)}$ as the cell tensor that is made up of γ $\mathbf{T}^{\text{cell}(1)}$'s, where γ is called the size of \mathbf{T}^{cell} . (b) If the u th bond of a \mathbf{T}^{cell} is connected with the v th bond of its adjacent \mathbf{T}^{cell} with $u \neq v$, then under the permutation operation between the u th and v th bonds, the \mathbf{T}^{cell} is required invariant, say $T^{\text{cell}}_{\dots \xi_u \dots \xi_v \dots} = T^{\text{cell}}_{\dots \xi_v \dots \xi_u \dots}$. We call the bonds ξ_u and ξ_v an index pair. When $u = v$, ξ_u forms a pair with itself.

For the spin-1/2 Heisenberg model on the infinite honeycomb lattice, we can rewrite Eq. (1) into the catalyzable form as $Z = g\text{Tr}(\prod_i \mathbf{T}^{\text{cell},i})$ with $T^{\text{cell},i}_{\xi_1 \xi_2 \xi_4 \xi_5} = \sum_{\xi_3} \mathcal{A}^i_{\xi_1 \xi_2 \xi_3} \mathcal{B}^i_{\xi_4 \xi_5 \xi_3}$, and

$$\mathcal{A}^i_{\xi_1 \xi_2 \xi_3} = \sum_{p_i p'_i \tilde{p}_i \tilde{p}'_i} A^i_{p_i p'_i g_1 g_2 g_3} \tilde{A}^i_{\tilde{p}_i \tilde{p}'_i \tilde{g}_1 \tilde{g}_2 \tilde{g}_3} \delta^i_{p_i \tilde{p}_i} \tilde{\delta}^i_{p'_i \tilde{p}'_i}, \quad (2)$$

$$\mathcal{B}^j_{\xi_4 \xi_5 \xi_6} = \sum_{p_j p'_j \tilde{p}_j \tilde{p}'_j} B^j_{p_j p'_j g_4 g_5 g_6} \tilde{B}^j_{\tilde{p}_j \tilde{p}'_j \tilde{g}_4 \tilde{g}_5 \tilde{g}_6} \delta^j_{p'_j \tilde{p}_j} \tilde{\delta}^j_{p_j \tilde{p}'_j}, \quad (3)$$

where the composite bond $\xi_a = (g_a, \tilde{g}_a)$ [Fig. 1 (a)]. The partition function is now represented as a square closed TN [Fig. 1 (b)]. In \mathbf{T}^{cell} , ξ_1 (ξ_2) forms an index pair with ξ_4 (ξ_5). Owing to the symmetry of the model, the permutation invariance is satisfied.

Now we introduce the catalyzers \mathbf{x}^α ($\alpha = 1, 2, \dots, J$ with J the number of index pairs) that are a set of unit-norm column vectors defined on a catalyzable TN formed by the n th-order \mathbf{T}^{cell} with following conditions: (a) Recursive condition. The catalyzers \mathbf{x}^α are the solutions of the set of self-consistent equations $\Gamma \mathbf{x}^\alpha_{\xi_a} = \sum_{\xi_1 \dots \xi_{a-1} \xi_{a+1} \dots} T^{\text{cell}}_{\xi_1 \xi_2 \dots} x^{\alpha_1}_{\xi_1} \dots x^{\alpha_{a-1}}_{\xi_{a-1}} x^{\alpha_{a+1}}_{\xi_{a+1}} \dots x^{\alpha_n}_{\xi_n}$ with Γ a positive constant for any $a = 1, \dots, n$. Henceforth, $\alpha_a = \alpha_b$ if a th and b th bonds form a pair. The \mathbf{T}^{cell} is considered as a nonlinear mapping $\mathcal{T}^{\text{cell}} : \prod_{a \neq b} \mathbb{V}^{\alpha_a} \rightarrow \mathbb{V}^{\alpha_b}$ with \mathbb{V}^{α_a} the vector space of \mathbf{x}^{α_a} . To describe the convergence of the mapping the Lyapunov exponent I^{lya} can be defined as

$$I^{\text{lya}} = \lim_{\Theta \rightarrow \infty} \sum_{\theta=1}^{\Theta} \left\{ \ln \sum_{a=1}^n \frac{|\mathcal{T}^\theta(\mathbf{x}^{\alpha_a}) - \mathcal{T}[\mathcal{T}^{\theta-1}(\mathbf{x}^{\alpha_a}) + \epsilon^{\alpha_a}]|}{n|\epsilon^{\alpha_a}|} \right\} / \Theta, \quad (4)$$

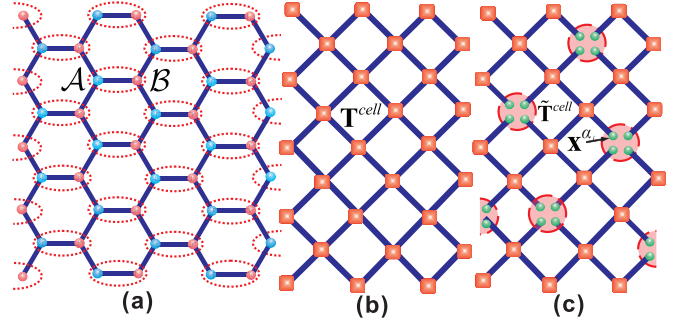


FIG. 1: (Color online) (a) The closed TN that is comprised of two inequivalent tensors \mathcal{A} and \mathcal{B} , which represents the partition function of the spin-1/2 Heisenberg antiferromagnet on the honeycomb lattice. (b) The catalyzable TN formed by \mathbf{T}^{cell} is obtained by contracting a common bond between \mathcal{A} and \mathcal{B} . (c) One possible configuration of the defective TN in which certain \mathbf{T}^{cell} 's are replaced by the rank-1 tensor $\tilde{\mathbf{T}}^{\text{cell}}$ to forbidden the loops formed only by \mathbf{T}^{cell} 's.

with ϵ^{α_a} the infinitesimal random vector and $\mathcal{T}^\theta = \mathcal{T}[\mathcal{T}(\dots)]$. (b) Optimization condition. The least-squares cost function $\mathcal{D} = \sqrt{\sum_{\xi_1 \xi_2 \dots} [T^{\text{cell}}_{\xi_1 \xi_2 \dots} - \prod_a x^{\alpha_a}_{\xi_a}]^2}$ is minimized [16]. An equivalent representation of the optimization condition is that the inner product function $\tilde{\Gamma} = \sum_{\xi_1 \xi_2 \dots} T^{\text{cell}}_{\xi_1 \xi_2 \dots} x^{\alpha_1}_{\xi_1} x^{\alpha_2}_{\xi_2} \dots > 0$ is maximized. From the optimization condition, the \mathbf{x}^{α_a} 's form the rank-1 decomposition of the \mathbf{T}^{cell} , namely $\mathbf{T}^{\text{cell}} \simeq \prod_a \mathbf{x}^{\alpha_a}$. In what follows, we shall show that the infinite contraction for the partition function as well as observables can be dramatically simplified in the framework mentioned above by approximating the catalyzable TN with defects. The loop character I^{loop} is thus proposed to display the validity of such an approximation.

The defective TN is obtained by replacing minimal number of \mathbf{T}^{cell} 's in the catalyzable TN with the rank-1 tensor $\tilde{\mathbf{T}}^{\text{cell}} = \prod_a \mathbf{x}^{\alpha_a}$, so that there exist no loops in the TN formed only by \mathbf{T}^{cell} [Fig. 1 (c)]. The $\tilde{\mathbf{T}}^{\text{cell}}$ is called a defect. Under this circumstance, the partition function Z of the prototype model in Eq. (1) is simplified as

$$Z = \tilde{\Gamma}^{\mathcal{N}-1} g\text{Tr}(\mathbf{T}^{\text{cell}} \tilde{\mathbf{T}}^{\text{cell}}) = \tilde{\Gamma}^{\mathcal{N}-1} g\text{Tr}(\mathbf{T}^{\text{cell}} \prod_a \mathbf{x}^{\alpha_a}) = \tilde{\Gamma}^{\mathcal{N}}, \quad (5)$$

with $\mathcal{N} \rightarrow \infty$ the number of the \mathbf{T}^{cell} 's. Equation (5) can be proved by reversing the infinite contraction procedure into an infinite growing one. From Eq. (5), the defective TN can be naturally rebuilt with minimal number of $\tilde{\mathbf{T}}^{\text{cell}}$'s. The recursive and optimization conditions are employed repeatedly to grow the TN and construct the $\tilde{\mathbf{T}}^{\text{cell}}$ with catalyzers, respectively. We illustrate a part of the growing procedure shown in Fig. 2 (a). It should be cautious that the defect reconstructed is $\tilde{\mathbf{T}}^{\text{cell}}_{\xi_a \xi_b \xi_c \xi_d}$, and the permutation invariance (restriction (b) of the catalyzable TN) is needed to ensure this defect is the rank-1 tensor of the original $T^{\text{cell}}_{\xi_a \xi_b \xi_c \xi_d}$. One may note that although there are many possible configurations for which cell tensors will be replaced by the defects, Eq. (5) holds so long as the loops of pure \mathbf{T}^{cell} 's are forbidden. Alternatively, one can be-

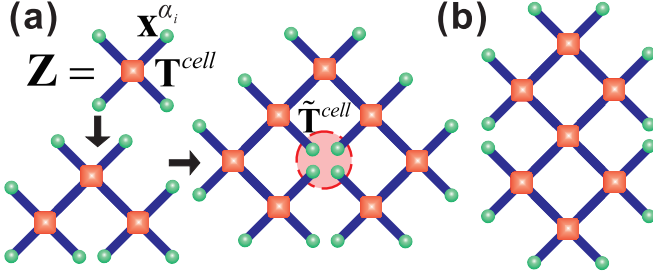


FIG. 2: (Color online) (a) A part of the growing procedure of the defective TN beginning from Eq. (5). The recursive condition is used to grow the TN and the optimization condition is used to construct the rank-1 tensor $\tilde{\mathbf{T}}^{cell}$ with \mathbf{x}^{α_i} 's. (b) One possible construction of the partition function with loops of $\mathbf{T}^{cell(1)}$'s.

gin with the catalyzers and a cluster of the cell tensors that already contains the loops of \mathbf{T}^{cell} 's [Fig. 2 (b)], and grow the rest, but in this case, Eq. (5) should be modified accordingly.

The thermal average of an operator $\hat{O}^{ij...k}$ can be similarly simplified within the NCD scheme. It can be noticed that, except the tensors that share the physical space with $\hat{O}^{ij...k}$, the rest of the TN are exactly the same as those of the partition function. We formally denote the cluster formed by tensors sharing the physical space with $\hat{O}^{ij...k}$ as $\Phi_{p_1...p_k p'_1...p'_k g_1...g_N}$. The average $\langle \hat{O}^{ij...k} \rangle$ can be obtained by

$$\begin{aligned} \langle \hat{O}^{ij...k} \rangle &= pTr[\hat{O}^{ij...k} gTr(\Phi \prod_{a=1}^N \mathbf{x}^{\alpha_a})]/Z \\ &= \sum_{\substack{p_1...p_k \\ p'_1...p'_k}} [O^{ij...k}_{p_1...p_k p'_1...p'_k} \sum_{g_1...g_N} (\Phi_{p_1...p_k p'_1...p'_k g_1...g_N} \prod_{a=1}^N x^{\alpha_a}_{g_a})]/Z. \end{aligned} \quad (6)$$

The approximation can be improved by increasing the size of the cell tensor. For the present HAF model, we can construct \mathbf{T}^{cell} through \mathbf{T}^\uparrow and \mathbf{T}^\downarrow :

$$\begin{aligned} T^{cell(\gamma)}_{(a_1 a_3)(b_3 b_4)(c_2 c_4)(d_1 d_2)} &= \sum_{a_2 a_4 b_1 b_2 c_1 c_3 d_3 d_4} T^{\uparrow \gamma_1}_{a_1 b_1 c_1 d_1} T^{\uparrow \gamma_1}_{a_2 b_2 c_2 d_2} T^{\downarrow \gamma_2}_{a_3 b_3 c_3 d_3} \\ &\quad T^{\downarrow \gamma_2}_{a_4 b_4 c_4 d_4} \delta_{a_2 c_1} \delta_{b_1 d_3} \delta_{a_4 c_3} \delta_{b_2 d_4}, \end{aligned} \quad (7)$$

with $\gamma = 2(\gamma_1 + \gamma_2)$. \mathbf{T}^\uparrow and \mathbf{T}^\downarrow are initiated as $\mathbf{T}^{cell(1)}$ and increased as $T^{\uparrow \gamma+1}_{(aa')b'(cc')d} = \sum_{bd'} T^{\uparrow \gamma+1}_{abcd} T^{cell(1)}_{a'b'c'd'} \delta_{bd'}$ and $T^{\downarrow \gamma+1}_{(aa')b(cc')d'} = \sum_{b'd} T^{\downarrow \gamma+1}_{abcd} T^{cell(1)}_{a'b'c'd'} \delta_{b'd}$, respectively. Note that this is not the only way to increase \mathbf{T}^{cell} 's size, but is the way that can preserve the symmetry of \mathbf{T}^{cell} with truncations at a reasonable cost. To see how the increase of γ improves the approximation, we introduce the “transfer matrix” of the partition function, $\mathcal{M}(\gamma) = gTr[T^{cell(\gamma)} \mathbf{x}^{\alpha_a, \gamma} \mathbf{x}^{\alpha_c, \gamma}]$. Thus we can simplify Z at large γ as $Z \simeq \lim_{l \rightarrow \infty} \tilde{T}^l Tr[\mathcal{M}(\gamma)^l]$, where the catalyzer $\mathbf{x}^{\alpha_{b(d)}, \gamma}$ is the dominant eigenvector of $\mathcal{M}(\gamma)$. On the other hand, as $\mathbf{x}^{\alpha_{b(d)}, \gamma}$ can be written in the form of a matrix product state (MPS) [17] with $(\gamma_1 + \gamma_2)$ “physical” bonds, we

may define the quasi-entanglement entropy (QEE) of the MPS as

$$S = - \sum_i (\mu_i^{b(d), \gamma})^2 \ln[(\mu_i^{b(d), \gamma})^2], \quad (8)$$

with $\mu_i^{b(d), \gamma}$ the normalized singular spectrum of the matrix $x^{\alpha_{b, \gamma}}_{b_3 b_4} (x^{\alpha_{d, \gamma}}_{d_1 d_2})$.

In addition, one can see that the defective TN with $\mathbf{T}^{cell(\gamma+1)}$'s and $\tilde{\mathbf{T}}^{cell(\gamma+1)}$'s contains more loops of $\mathbf{T}^{cell(1)}$ than that with $\mathbf{T}^{cell(\gamma)}$'s and $\tilde{\mathbf{T}}^{cell(\gamma)}$'s (recall that in this defective TN, loops of pure $\mathbf{T}^{cell(\gamma)}$'s, not $\mathbf{T}^{cell(1)}$'s, are forbidden). In this way, we can choose the catalyzers of the unchanged bonds b and d to define the loop character I^{loop} as

$$I^{loop(\gamma)} = 1 - (\mathbf{x}^{\alpha_{b(d)}, \gamma+1})^T \mathbf{x}^{\alpha_{b(d)}, \gamma}, \quad (9)$$

with $\mathbf{x}^{\alpha_{i, \gamma}}$ the catalyzers of $\mathbf{T}^{cell(\gamma)}$. Such a character I^{loop} quantifies the loop dependence of the TPDO. It is worth mentioning that while I^{lya} delineates the properties of a certain mapping, I^{loop} describes the difference between two mappings with different cell tensor sizes. Specifically, when $I^{loop(\gamma)}$ converges to zero as γ increases, the effects from larger loops are negligible. So, $I^{loop(\gamma)}$ can be used to monitor the error brought by the defective TN approximation.

The dimensions of the cell tensor's bonds a and c are enlarged during the growing procedure while those of the bonds b and d are unchanged. The truncation to bound the dimension is the same as the way to bound the dimension of the geometrical bond of the TPDO during the imaginary time evolution, as will be introduced later.

The power algorithm for catalyzers.— We employ the power algorithm [16] to calculate the catalyzers of \mathbf{T}^{cell} . The \mathbf{x}^{α_i} is renewed alternately until its convergence by

$$\mathcal{T}^{cell}(\mathbf{x}^{\alpha_1(t+1)}, \dots, \mathbf{x}^{\alpha_{i-1}(t+1)}, \mathbf{x}^{\alpha_{i+1}(t)}, \dots) \rightarrow \mathbf{x}^{\alpha_i(t+1)} \quad (10)$$

with t the iteration times. The Lyapunov exponent I^{lya} can be utilized to describe the property of convergence for a given \mathbf{T}^{cell} . In particular, for a given convergence with smaller I^{lya} less iteration times are needed, and vice versa. Notice that one iteration step for the catalyzers with the mapping (10) is actually equivalent to growing one \mathbf{T}^{cell} in the defective TN picture. In other words, the longer time to converge is equivalent to the contraction of a larger defective TN. Thus, an interesting meaning of I^{lya} in the NCD is that it indicates the “spatial-dependence” of the wave function with its local tensor representation. In our calculations, I^{lya} keeps negative for all parameter ranges. For I^{lya} being zero or positive, the system might have possible bifurcations or chaos.

The imaginary-time-sweep algorithm.— For the TPDO at finite temperature, we propose the imaginary-time-sweep algorithm (ITSA) based on the NCD scheme. First, we introduce the truncation principle for the enlarged bonds. Denote the bond to be truncated as \tilde{g} with its dimension $\tilde{\chi}$ and define the matrix \mathbf{M} such that $Z = \sum_{\tilde{g}\tilde{g}'} \delta_{\tilde{g}\tilde{g}'} M_{\tilde{g}\tilde{g}'} = Tr(\mathbf{M})$, which is obtained by simply contracting all shared bonds in Eq.(1)

except \tilde{g} . According to the linear algebra, the best truncation of the bond \tilde{g} can be reached using the singular value decomposition (SVD) on \mathbf{M} , say $\mathbf{M} \simeq \mathbf{P}\mathbf{A}\mathbf{Q}^T$, where only χ largest singular values and the corresponding left and right singular vectors are kept. Here χ is the preset dimension cut-off. The truncation error can be controlled by

$$\varepsilon = \left(\sum_{a=\chi+1}^{\tilde{\chi}} \Lambda_a \right) / \left(\sum_{a=1}^{\tilde{\chi}} \Lambda_a \right). \quad (11)$$

Redefining the matrix as $\tilde{\mathbf{M}} = \sqrt{\Lambda}\mathbf{P}^T\mathbf{Q}\sqrt{\Lambda}$, we have $Z = \text{Tr}(\tilde{\mathbf{M}})$, and then, use the SVD again to decompose $\tilde{\mathbf{M}}$ as $\tilde{\mathbf{M}} = \tilde{\mathbf{P}}\tilde{\Lambda}\tilde{\mathbf{Q}}^T$. The best $\tilde{\chi} \times \chi$ truncation matrices for bonds \tilde{g} and \tilde{g}' are obtained by

$$\tilde{\mathbf{P}} = \mathbf{P}\Lambda^{-1/2}\tilde{\mathbf{P}}\sqrt{\tilde{\Lambda}}, \quad \tilde{\mathbf{Q}} = \mathbf{Q}\Lambda^{-1/2}\tilde{\mathbf{Q}}\sqrt{\tilde{\Lambda}}, \quad (12)$$

such that $\delta = \tilde{\mathbf{P}}\tilde{\mathbf{Q}}^T$ (δ is the Dirichlet matrix). Thus, as long as we have \mathbf{M} , we can get the best truncation matrices. Obviously, the difficulty in obtaining \mathbf{M} is as big as in calculating Z itself. To simplify the calculation of \mathbf{M} , we may adopt the defective TN scheme of the NCD in the way of

$$\frac{M_{g_i g'_i}}{\tilde{\Gamma}^N} = \begin{cases} \sum_{g''} x_{g_i g''}^j x_{g'' g'_i}^j \\ \sum_{\xi_a \xi_b \xi_c \xi_d \xi_f \xi_g} \mathcal{A}_{\xi_a \xi_b \xi_c \xi_d \xi_f \xi_g}^i \mathcal{B}_{\xi_d \xi_f \xi_g \xi_a \xi_b \xi_c}^j x_{\xi_a \xi_b}^a x_{\xi_b \xi_c}^b x_{\xi_c \xi_d}^c x_{\xi_d \xi_f}^d / \tilde{\Gamma}, \end{cases} \quad (13)$$

where we write selectively the composite index ξ_i into (g_i, g'_i) for clarity. The first line of the *r.h.s.* of Eq. (13) holds when the enlarged bond is one of \mathbf{T}^{cell} 's bonds, and the second line holds when the enlarged bond is contracted in the construction of \mathbf{T}^{cell} . Equation (13) can be proved by infinitely growing the defective TN, similar to that for calculating the observables.

There are two main parts of the ITSA (Fig. 3), initialization and sweeping procedure. In the initialization part, each TPDO at the inverse temperature $\beta \leq \tilde{\beta}$ is initialized ($\tilde{\beta}$ is the targeted temperature). The M is calculated with the partition function $Z(2\beta)$ constructed by the TPDO $\hat{\rho}(\beta)$ and its copy, where β that begins from τ is the inverse temperature of the present TPDO. In the sweeping part, the M for each truncation is obtained from the partition function $Z(\tilde{\beta})$, i.e. when the TPDO is evolved to β , denoted as $\hat{\rho}(\beta)$, $Z(\tilde{\beta})$ can be constructed with $\hat{\rho}(\beta)$ and the pre-obtained $\hat{\rho}(\tilde{\beta} - \beta)$. If it is the first sweep for this targeted temperature $\tilde{\beta}$, we can construct $Z(\tilde{\beta})$ using $\hat{\rho}(\tilde{\beta} - \beta)$ saved in the initialization, otherwise using $\hat{\rho}(\tilde{\beta} - \beta)$ obtained in the last sweeping step.

The errors in the ITSA come from three parts: the error from the Trotter-Suzuki decomposition, the truncation error and the error caused by introducing the defects (rank-1 tensors). The first part is controlled by τ , and the second is controlled by ε [Eq. (11)]. The third part affects the calculations of transformation matrices and observables, and a possible choice to control it is the cost function \mathcal{D} (that is in fact the error of the single tensor rank-1 approximation). But considering that the contribution from the “residual” tensor $\mathbf{T}^{cell} - \tilde{\mathbf{T}}^{cell}$ may vanish along with the infinite tensor product,

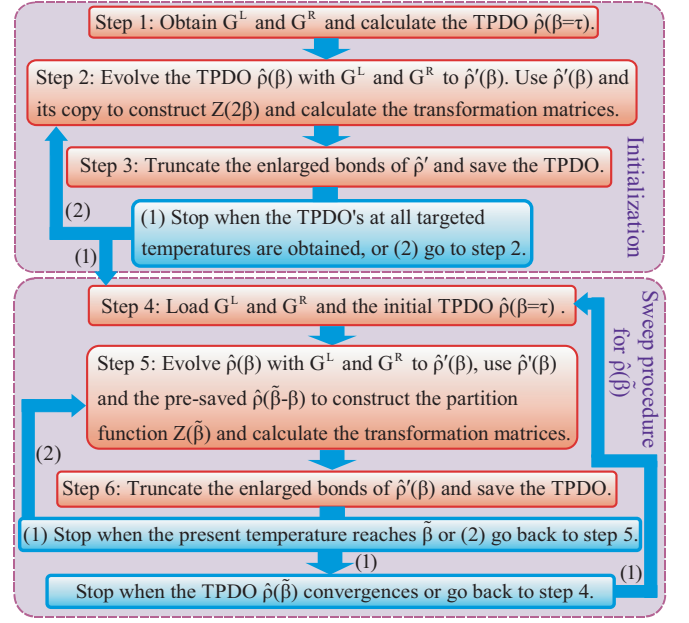


FIG. 3: (Color online) The sketch of the ITSA algorithm.

the loop character I^{loop} is a more solid choice to control the defect-caused error.

Applications to the spin-1/2 Heisenberg antiferromagnet on honeycomb lattice.—To show the efficiency and accuracy of the NCD approach, we take the spin-1/2 Heisenberg antiferromagnet on honeycomb lattice with nearest neighbor interactions as an example, whose local Hamiltonian reads $\hat{H}^{ij} = \Delta[\hat{S}^{i(x)}\hat{S}^{j(x)} + \hat{S}^{i(y)}\hat{S}^{j(y)}] + \hat{S}^{i(z)}\hat{S}^{j(z)}$, where Δ characterizes the anisotropy of exchange interactions. First, we calculate the energy per site $E = \text{Tr}(\hat{H}_{ij}\hat{\rho})$ at $\Delta = 0.5$ and 1 to testify the validity of NCD [Fig. 4 (a)]. The translation invariance has been used. The results are compared with QMC simulations, in which different dimension cut-offs χ are used in the NCD calculations. We use the tensor cluster in Fig. 2 (b) to calculate the truncation matrices, where the truncation error ε is found around 10^{-5} . The iteration in the power algorithm is stopped when the difference of the catalyzers at t and $t+1$ steps [Eq. (10)] is less than 10^{-14} . In calculating the observables within the NCD, the loop character I^{loop} is required under 10^{-7} and the cell tensor size is increased until the difference of between the observables with size γ and $\gamma+2$ is less than 10^{-6} . We set the lattice size as 64×64 for QMC calculations and keep the errors around 10^{-5} . For the characters of the TNS, we fix the cell tensor size $\gamma = 500$ and set $\Theta = 300$ [Eq. (4)] for I^{ba} .

It is known that in the present system a thermodynamic phase transition (TPT) may occur in the presence of the spin anisotropy Δ , and the critical temperature can be determined by the divergent peak of specific heat $C = -\beta^2 dE/d\beta$. Our calculation of C shows that the TPT occurs at $T^C = 0.345$ with $\Delta = 0.5$ [Fig. 4 (b)] for both NCD and QMC calculations. We also calculated the QEE [Eq. (8)], where the similar behavior near the critical point is observed [Fig. 5 (a)]. The sharp peak of S appears at $T^S = 0.3610$, close to the value

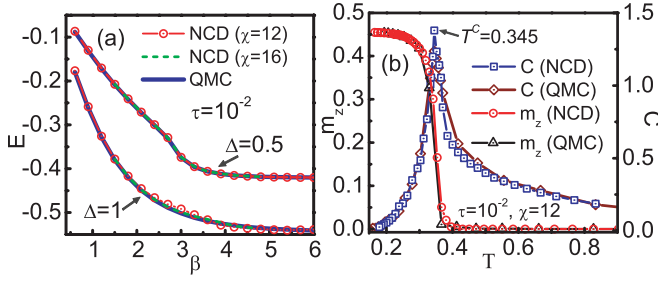


FIG. 4: (Color online) (a) Energy per site E obtained by NCD and QMC at $\Delta = 0.5$ and 1 . (b) The staggered magnetization per site m_z and the specific heat C as functions of temperature T for $\Delta = 0.5$. The specific heat indicates a thermodynamic phase transition at $T^C = 0.345$.

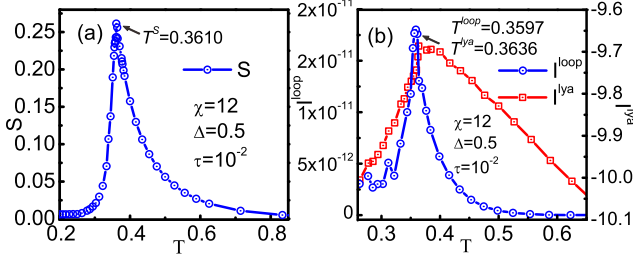


FIG. 5: (Color online) (a) The temperature dependence of the QEE S , in which the critical temperature $T^S = 0.3610$. (b) The temperature dependence of the Lyapunov exponent and the loop character, which show sharp peaks at $T^{lya} = 0.3636$ and $T^{loop} = 0.3597$, respectively.

obtained from the specific heat. The QEE vanishes (about $10^{-3} \sim 10^{-4}$) when the temperature is away from the critical vicinity.

We studied the T -dependence of the Lyapunov exponent I^{lya} [Eq. (4)] and the loop character I^{loop} [Eq. (9)]. The results [Fig. 5 (b)] show that the characters reach maximum at $T^{lya} = 0.3636$ and $T^{loop} = 0.3597$, again close to the critical temperatures obtained from the specific heat and the QEE. I^{lya} shows that the TPDO near the critical point has the property of considerably strong spatial-dependence, suggesting that the TPDO could be well approximated with a defective TN of great size. From I^{loop} one may observe that the TPDO bears high loop dependence and the effects from the loops of cell tensors can be ignored only when the size of cell tensor γ is large enough. Meanwhile, noticing that the QEE versus T behaves differently in different phases, showing promisingly a prospective development of NCD, that is, the phases can be classified by the behavior of the QEE. When the temperature is away from the critical point, the whole TN can be approximated by a relatively small defective TN, where the effects from the loops of cell tensors can be ignored at relatively small size. It should be remarked that as it is difficult for a TNS to approximate the state in the critical vicinity [18], it is expected that with sufficient large χ , the critical temperatures determined by the specific heat and the characters S , I^{lya}

and I^{loop} will be coincident.

In conclusion, we developed the NCD for exploring the thermodynamic properties of 2D quantum lattice models, and proposed the ITSA that is free from the negative sign problem for the numerical realization of NCD. The calculated results for the spin-1/2 HAF on honeycomb lattice as an example are found consistent well with the QMC simulations. New characters such as the quasi-entanglement entropy, Lyapunov exponent and loop character are suggested to describe properties of the thermal states and detect possible thermodynamic phase transitions of the system. The possible extension of the NCD to other quantum lattice systems can be done in a straightforward way.

The authors are indebted to W. Li, X. Yan, Y. Zhao, Z. C. Wang and Q. R. Zheng for stimulating discussions. This work is supported in part by the NSFC (Grants No. 90922033 and No. 10934008), the MOST of China (Grant No. 2012CB932900 and No. 2013CB933401), and the CAS.

* Corresponding author. Email: gsu@ucas.ac.cn

- [1] H. L. Stormer, H. L. Stormer and A. C. Gossard, Rev. Mod. Phys. **71**, 298 (1999).
- [2] L. Balents, Nature **464**, 199 (2010).
- [3] G. Vidal, J. I. Latorre, E. Rico, and A. Kitaev, Phys. Rev. Lett. **90**, 227902 (2003); T. R. de Oliveira, G. Rigolin, M. C. de Oliveira, and E. Miranda, Phys. Rev. Lett. **97**, 170401 (2006); L. Amico, R. Fazio, A. Osterloh and V. Vedral, Rev. Mod. Phys. **80**, 517 (2008).
- [4] P. Zanardi, H. T. Quan, X. G. Wang, and C. P. Sun, Phys. Rev. E **75**, 032109 (2007); H. Q. Zhou, R. Orús, and G. Vidal, Phys. Rev. Lett. **100**, 080601 (2008); S. Garnerone, D. Abasto, S. Haas, and P. Zanardi, Phys. Rev. A **79**, 032302 (2009); M. M. Rams and B. Damski, Phys. Rev. Lett. **106**, 055701 (2011).
- [5] S. R. White, Phys. Rev. Lett. **69**, 2863 (1992), Phys. Rev. B **48**, 10345 (1993).
- [6] S. R. White and A. E. Feiguin, Phys. Rev. Lett. **93**, 076401 (2004); A. E. Feiguin and S. R. White, Phys. Rev. B **72**, 220401(R) (2005).
- [7] S. R. White and D. J. Scalapino, Phys. Rev. Lett. **80**, 1272 (1998).
- [8] F. Verstraete and J. I. Cirac, arXiv:cond-mat/0407066; J. Jordan, R. Orús, G. Vidal, F. Verstraete, and J. I. Cirac, Phys. Rev. Lett. **101**, 250602 (2008).
- [9] H. C. Jiang, Z. Y. Weng, and T. Xiang, Phys. Rev. Lett. **101**, 090603 (2008); Z. Y. Xie, H. C. Jiang, Q. N. Chen, Z. Y. Weng, and T. Xiang, Phys. Rev. Lett. **103**, 160601 (2009).
- [10] Z. C. Gu, M. Levin, and X. G. Wen, Phys. Rev. B **78**, 205116 (2008); Z.C. Gu and X. G. Wen, Phys. Rev. B **80**, 155131 (2009).
- [11] G. Vidal, Phys. Rev. Lett. **99**, 220405 (2007); Phys. Rev. Lett. **101**, 110501 (2008).
- [12] E. M. Stoudenmire and S. R. White, Annual Review of Condensed Matter Physics, **3**: 111-128 (2012).
- [13] J. I. Cirac and F. Verstraete, J. Phys. A: Math. Theor. **42**, 504004 (2009).
- [14] M. Suzuki and M. Inoue, Prog. Theor. Phys. **78**, 787 (1987); M. Inoue and M. Suzuki, Prog. Theor. Phys. **79**, 645 (1988).
- [15] S. J. Ran, W. Li, B. Xi, Z. Zhang, and G. Su, Phys. Rev. B **86**,

- 134429 (2012).
- [16] L. De Lathauwer, B. De Moor, and J. Vandewalle, *SIAM. J. Matrix Anal. and Appl.* **21**, 1324-1342 (2000).
 - [17] U. Schollwöck, *Anal. of Phys.* **326**, 96 (2011) and references therein.
 - [18] The related discussions for an MPS to describe the state in the critical vicinity are in L. Tagliacozzo, T. R. de Oliveira, S. Iblisdir, and J. I. Latorre, *Phys. Rev. B* **78**, 024410 (2008); F. Pollmann, S. Mukerjee, A. M. Turner, and J. E. Moore, *Phys. Rev. Lett.* **102**, 255701 (2009).